BB

TRI-PP-87-79
Oct 1987

GAMOW–TELLER STRENGTH FUNCTIONS FROM NUCLEON SCATTERING EXPERIMENTS

O. Häusser
Simon Fraser University, Burnaby,B.C., Canada V5A 1S6
and
TRIUMF, 4004 Wesbrook Mall, Vancouver, B.C., Canada V6T 2A3

ABSTRACT

The spin–isospin structure of nuclear excitations up to ~ 50 MeV has been studied using (n,p), (p,p′) and (p,n) reactions at TRIUMF. At 200–400 MeV the L = 0 isovector spin-transfer component of the cross section is closely related to the Gamow-Teller strength function. Results are discussed which have implications for Gamow–Teller quenching in (sd) and (fp) shell nuclei, for the Ikeda sum rule, and for the importance of 2particle-2hole correlations in nuclear wavefunctions.

INTRODUCTION

It is well known that in nuclear β decay Fermi strength (quantum numbers L = 0, S = 0, $T_i = T_f \neq 0$) is concentrated in a single transition, whereas Gamow-Teller (GT) strength (L = 0, S = 1, T = 1) is spread over a wide energy region as a result of the spin–dependent residual nuclear interaction. Studies of β decays in nuclei far from stability offer the opportunity to examine a large energy window and thus a large fraction of the total GT strength. Unfortunately, mixing of 2particle-2hole (2p2h) into (1p1h) states [1], or coherent isobar-hole admixtures [2] may produce a shift of GT strength to energies considerably above 10 MeV, making it undetectable in conventional β decay experiments.

Nucleon (N) scattering experiments at intermediate energies can be used to provide a substitute and extension of GT studies in beta decay. Pioneering work [3, 4] using the time-of-flight setup at Indiana University (IUCF) has demonstrated that the (p,n) reaction, at $E_p = 120 - 200$ MeV and small momentum transfer, can be quantitatively related to GT strength known from analogous β decay. We discuss here results of (n,p), ($\vec{p},\vec{p}'$) , and (p,n) experiments carried out at 200–400 MeV using the medium-resolution spectrometer (MRS) at TRIUMF. Recent modifications of the MRS include the installation of a dispersion-matching system, of a focal-plane polarimeter [5] to analyze the transverse spin components of scattered protons, and of a compact sweeping magnet which is part of the CHARGEX facility [6, 7] for the study of (n,p) and (p,n) reactions. Although the resolution achieved is modest (typically 140 keV FWHM in (p,p′) and 1 MeV in charge exchange reactions) this is compensated for by the extreme selectivity of these reactions to excite nuclear spin-isospin modes. The optimum sensitivity occurs near 300 MeV, where multistep processes are less important than at lower energies. The relationship between nucleon scattering and β decay is shown in Table 1.

Table I Nucleon scattering and beta decay

reaction	transition operator	GT strength	total strength	isospin of final state	σ/B(GT) calibrated in
(p,n)	$\sigma\tau_-$	B(GT$_-$)	S$_-$	$T_0 - 1$, T_0, $T_0 + 1$	β^+ decay
($\vec{p},\vec{p}'$)	$\sigma\tau_0$			T_0, $T_0 + 1$	
(n,p)	$\sigma\tau_+$	B(GT$_+$)	S$_+$	$T_0 + 1$	β^- decay

Invited paper presented at the 5th International Conference on Nuclei far from Stability, September 14-19, 1987, Lake Rosseau, Ontario, Canada.

TRI - PP 87-79
·9

The combination of (p,n) and (n,p) reactions makes possible tests of the Ikeda sum rule [8], $S_- - S_+ = 3(N - Z)$, which might be violated if GT strength is shifted outside of the energy window over which the GT strength is summed. For targets with ground state isospin $T_0 \neq 0$ the spin response for individual isospin components ($T_0 - 1, T_0, T_0 + 1$) can be constructed by combining the results from all three reactions. Such a program has been carried out for the $T_3 = 1$ nucleus ^{54}Fe. The experiments were performed in collaboration with R. Abegg, P. Alford, A. Celler, D. Frekers, R. Helmer, R. Henderson, K. Hicks, P. Jackson, R. Jeppesen, A. Miller, M. Moinester, K. Raywood, R. Sawafta, M. Vetterli and S. Yen. The Rutgers group which includes C. Glashausser, R. Fergerson, and K. Jones has made substantial contributions to the ^{54}Fe($\vec{p},\vec{p}'$) experiment.

CONVERTING CROSS SECTIONS INTO GT STRENGTH.

The proportionality between nucleon scattering cross sections and GT strength is expected to hold at small momentum transfers in the framework of the single–step distorted wave impulse approximation (DWIA). Assuming an (n,p) reaction for which B(GT$_-$) (and thus B(GT$_+$)) is known from corresponding β^- transitions, the cross section can be written (similar expressions are valid for (p,p′) and (p,n) reactions) as

$$\frac{d\sigma_{np}}{d\Omega}(q=0) = (\frac{\mu}{\pi\hbar^2})^2 \frac{k_i}{k_f} N^D_{\sigma\tau} |J_{\sigma\tau}|^2 B_\uparrow(GT_+)$$

$$B(GT_+) = \frac{1}{(2J_i+1)}[< J_f T_f | \Sigma\sigma\tau_+ | J_i T_i >]^2$$

$$B_\uparrow(GT_+) = \frac{(2J_f-1)}{(2J_i-1)} B_\downarrow(GT_-) = \frac{(2J_f-1)}{(2J_i-1)} (\frac{g_A}{g_V})^{-2} \frac{6163.4 \pm 3.8 sec}{ft}$$

In these expressions μ is the relativistic reduced energy divided by c^2, k_i and k_f are wave numbers, $g_A/g_V = 1.26$ is the ratio of axial vector and vector coupling constants, and $J_{\sigma\tau}$ is the volume integral of the ($\sigma\tau$) component of the NN interaction. We do not make use of this factorized form of the cross section but employ instead a computer code which also includes spin-orbit and tensor pieces of the NN interaction. The distortion factor $N^D_{\sigma\tau}$ represents the difference between plane waves and distorted waves and reduces the cross section more and more as the target mass increases (typically by ~ 12% for A = 12 and a factor of three for A = 54). In most cases we have determined the distortions by extensive measurements of elastic scattering for the appropriate target and energy.

So far we have performed (n,p) calibration experiments [9] at 200 MeV for targets of ^{6}Li and ^{12,13}C. Figure 1 shows (n,p) spectra for targets of C (top) and CH$_2$ (bottom). Both spectra were obtained simultaneously using segmented targets separated by active wire chambers [7]. In the C spectrum (top) the large peak at Q = −12.6 MeV arises from the GT transition to the ^{12}B ground state (B(GT$_-$) = 0.999 ± 0.005 from ^{12}B β^- decay). The small peak at Q = 0 in the top spectrum arises from hydrogen in the mylar foils and the counter gas of the segmented target chamber. We obtain $\sigma_{np}(0°, q = 0)/B(GT) = 9.42 \pm 0.31$ mb/sr in good agreement, but more accurate than, previous IUCF results [4] for ^{12}C(p,n) at 200 MeV. This, and values for other pure GT transitions [9] in ^{6}Li(p,n) and ^{13}C(n,p), can be reproduced with an accuracy of 10% or better in DWIA calculations using as ingredients optical potentials derived from elastic scattering data, the effective NN interaction (essentially $J_{\sigma\tau}$) of Franey and Love [10], and transition densities from microscopic shell model calculations. The GT values quoted in the following were obtained using σ/B(GT) calculated with the DWIA and may be subject to slight revisions as more calibration experiments will be carried out.

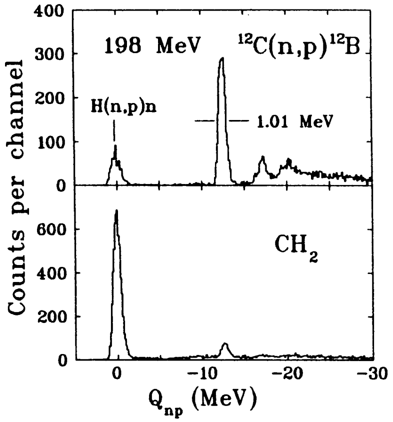

Fig. 1. (n,p) spectra obtained with a 198 MeV neutron beam and targets of carbon and CH_2.

Confirmation that the Franey–Love interaction describes well the energy-dependence of GT cross sections in the 200—400 MeV region comes from angular distribution measurements for the $^{28}Si(p,p')$ reaction leading to pure $1^+, T = 1$ states [11]. It is found that the 'quenching factors' f(p,p') required to bring experimental and calculated DWIA angular distributions into agreement do not vary appreciably (to an experimental uncertainty of ~ ±6%) at five incident proton energies between 200 and 400 MeV.

GAMOW-TELLER QUENCHING IN (sd) SHELL NUCLEI

Large-scale shell model calculations (WB [12] and WC [13]) provide comprehensive predictions of GT strength at low excitations in most (sd) shell nuclei. We have completed experiments [14] on the $^{26}Mg(n,p)^{26}Na$ reaction at 200 MeV and on inelastic proton scattering in ^{24}Mg at 250 MeV and in ^{28}Si at several energies [15, 11]. In the (p,p') reaction transitions to the 1^+, $T = 1$ states are analogs of transitions excited in the charge exchange reactions. A spectrum for $^{24}Mg(\vec{p},\vec{p}')$ and $\theta_{lab} = 2.9°$ is shown in the upper panel of Figure 2. The unwanted $S = 0$ component in the cross section can be eliminated by measurements of the spin-transfer probability S_{nn} using the focal plane polarimeter to detect a change in the proton polarization after scattering.

This is shown in the spin-transfer spectrum of Figure 2 (middle) where natural parity states with $S = 0$ are absent. The spin-transfer cross section σS_{nn} is thus a measure of the spin transfer strength in ^{24}Mg. The $L = 0$, GT components in the σS_{nn} spectra can be identified from their rapid decrease with increasing momentum transfer (e.g. compare the strong 1^+, $T = 1$ peak at 10.71 MeV excitation in the middle and lower spectra). The running sum of GT strength versus excitation energy in $^{24}Mg(\vec{p},\vec{p}')$ is compared in Figure 3 with predictions using WB [12] and WC [13] transition densities. It is apparent that both shell models give reasonably consistent estimates for the integrated GT strength but are less reliable for individual states. From the σS_{nn} data in ^{24}Mg between E_{exc}=9–15 MeV we deduce [15] an overall 1^+ quenching factor $< f(p,p') >= 0.80 \pm 0.10$. The error arises from counting statistics and uncertainties in the $L = 0$ fraction of σS_{nn} , but excludes systematic uncertainties in the average of WC and WB transition densities and in the ratio σ/B(GT).

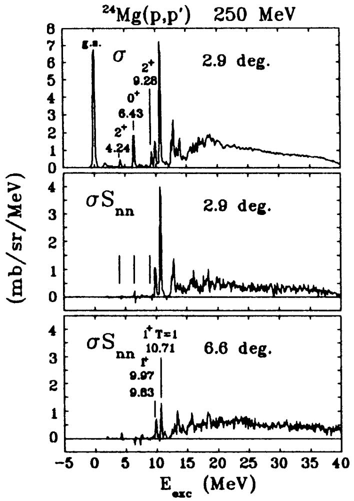

Fig. 2. Differential cross sections σ and spin-flip cross sections σS_{nn} for inelastic proton scattering from ^{24}Mg at 250 MeV.

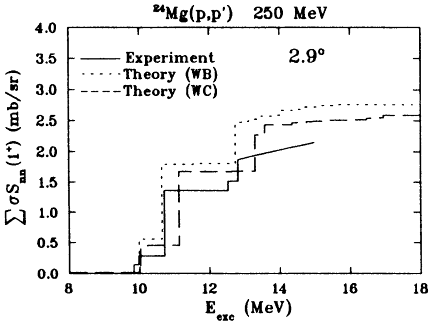

Fig. 3. Running sum of 1^+ spin-transfer strength for $^{24}Mg(\vec{p},\vec{p}')$ at 250 MeV and $\theta =$ 2.9°.

In ^{28}Si between E_{exc}=9-14 MeV we arrive [11] at an average 1^+,T = 1 quenching factor $< f(p,p') >=0.89 \pm 0.09$. These GT quenching factors are somewhat larger than those for charge exchange reactions in neighbouring nuclei [14, 16] ($f \approx 0.67$ for $^{26}Mg(n,p)$ and $f \approx 0.57$ for $^{26}Mg(p,n)$). The variation in the individual values for f beyond experimental errors may be attributed to uncertainties in the DWIA calculations for three reactions at different energies, to different integration intervals and analysis procedures, and to systematic uncertainties in the various transition densities.

THE SPIN–ISOSPIN RESPONSE OF ^{54}Fe.

The (n,p), ($\vec{p},\vec{p}'$), and (p,n) reactions on ^{54}Fe have recently been measured at TRIUMF near 300 MeV. Analysis of these reactions [17, 18] has resulted in a decomposition of the nuclear response for ^{54}Fe into spin and isospin components, and in a test of the Ikeda sum rule (see next section). Data have been obtained at 0-12° for (n,p), 3-15° for ($\vec{p},\vec{p}'$), and 0-15° for (p,n) reactions. Since in nucleon scattering different L-transfers peak at distinctly different angles, a decomposition into multipoles ($L = 0,1,2,...$) can be carried out. This is demonstrated in Figure 4 where the $L = 0,1,2$ components of (n,p) angular distributions [17] are shown for different excitation energies. The GT ($L = 0$) component is strongly peaked at 0° and is shown in Figure 5 for the three reactions. In ^{54}Fe($\vec{p},\vec{p}'$) at the most forward angle feasible in the experiment (3.1°) the M1 resonance at 9-15 MeV is seen much more clearly in the spin–transfer cross section σS_{nn} than in the cross section σ. For the (p,p′) reaction the $L = 0$ component in σS_{nn} above $E_x = 20$ MeV is rather uncertain and has been omitted in the plot.

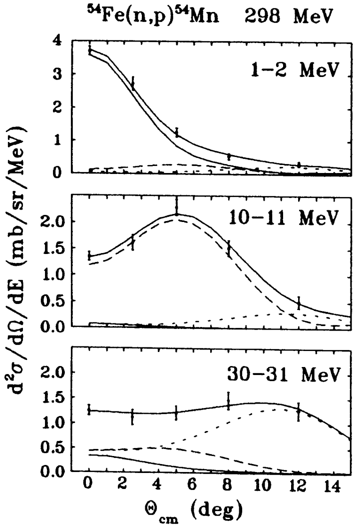

Fig. 4. Multipole decomposition of angular distributions for the ^{54}Fe(n,p)^{54}Mn reaction at three different excitation energies in ^{54}Mn. Solid lines: total and $L = 0$ part; dot-dashed lines: $L = 1$ part; short-dashed lines: $L = 2$ part.

The GT strength is concentrated at lower excitations, although the fitting procedure produces also a long GT tail to higher excitations. The intensity of this tail is however subject to large uncertainties since the GT fraction is small and depends on the small–angle behaviour of the $L = 1,2..$ angular distributions used in the decomposition. Such a tail would be expected from admixtures of (2p2h) components in the wavefunction [1] and would provide an explanation for the quenching of GT strength at low excitations.

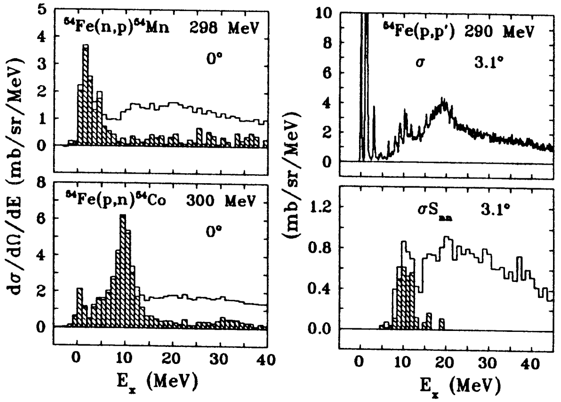

Fig. 5. Forward-angle spectra for (n,p) (top left), (p,n) (bottom left) and (p,p') (right) reactions on ^{54}Fe. The hatched areas correspond to the $L = 0$ (GT) components deduced from multipole decompositions.

In Table 2 we show the $L = 0$ component of the cross sections (or of σS_{nn}) for the three reactions, and quenching factors f based on the DWIA value of $\sigma_{np}(0°, q = 0)/B(GT) = 3.5$ mb/sr. The (p,n) result which is still preliminary is larger but statistically more accurate than that of Rapaport *etal* [19] obtained at 160 MeV. The quenching factors shown are for two extreme models, one in which a simple $(f_{7/2}^{14})$ ^{54}Fe ground state is assumed (f_A), and one in which RPA corrections have been estimated from a calculation in ^{60}Ni [20] (f_{RPA}). It is seen that GT quenching depends strongly on the assumptions about the Fermi surface, especially for the (n,p) reaction which tends to be Pauli blocked. In the (sd) shell where $0\hbar\omega$ configuration mixing is included fully no such asymmetry in the GT quenching factors for (p,n) and (n,p) has been observed.

Table II GT quenching factors in ^{54}Fe

reaction	E_{beam} (MeV)	measured quantity	angle (deg.)	$E_x^i \rightarrow E_x^f$ (MeV)	$L = 0$ strength (mb/sr)	f_A	f_{RPA}
(n,p)	298	σ	0	0 → 10	12.9	0.37	0.65
($\vec{p},\vec{p}'$)	290	σS_{nn}	3.1	4.5→ 14.5	2.8	0.39	~ 0.60
(p,n)	300	σ	0	0→ 13.5	33[a]	0.59[a]	0.77[a]

[a] preliminary value

Evidence for the importance of (2p2h) components in the wavefunctions is contained in the data at larger momentum transfers. At $q > 1 fm^{-1}$ giant resonances are no longer apparent and the nucleus can be approximated by the response of a semi-infinite slab [21, 22]. In Figure 6 we show large-angle (n,p) cross sections and σS_{nn} in (p,p′) together with calculations by Smith [22] which include the free NN response (long-dashed curves), the (1p1h) RPA response (short-dashed curves) and the combined (2p2h) (1p1h) RPA reponse (solid curves). The (2p2h) correlations push spin–transfer strength towards higher energies, an effect familiar from discussions of GT quenching [1]. The (2p2h) correlations bring about reasonable agreement for (n,p), whereas the $(\vec{p},\vec{p}')$ experiment demands even more spin–transfer strength above 30 MeV.

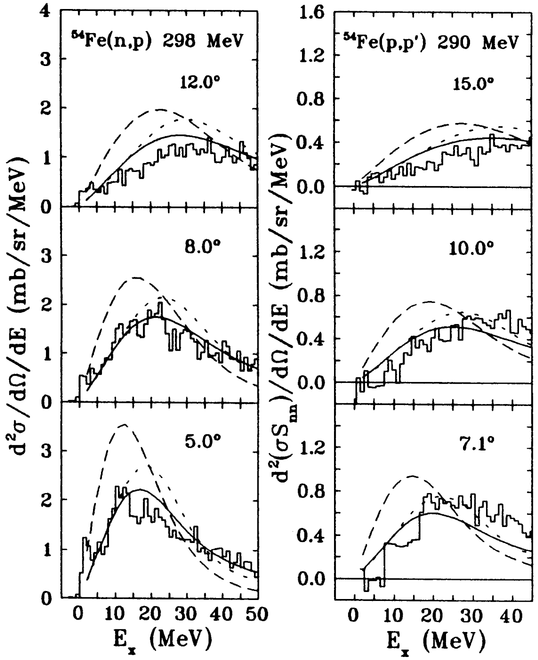

Fig. 6. Comparison between experimental (n,p) cross sections (left) and (p,p′) spin-flip cross sections (right) and predictions of the RPA surface response model of Smith [22]. The curves shown correspond to the free quasielastic response (long-dashed lines), the (1p1h) RPA (short-dashed lines), and to the RPA which includes (2p2h) correlations (solid lines).

TESTS OF THE IKEDA SUM RULE

From the L = 0 strength for the (n,p) and (p,n) reactions in Table 2 we obtain for the sum rule in ^{54}Fe a (still preliminary) value of $S_- - S_+ = 5.8 \pm 0.8$, which is nearly the full value of 6.

Another test of the sum rule was carried out in ^{90}Zr where a multipole decomposition of the experimental (p,n) spectrum [23] has found most of the GT sum rule, and where the data are well reproduced by RPA calculations [24] which include (2p2h) correlations and a correction for two-step processes. However, if a significant amount of S_+ strength were to be found in the (n,p) reaction the sum rule would still be violated, making room for the isobar-hole quenching mechanism [2]. In Figure 7 we show spectra for the ^{90}Zr(n, p)^{90}Y reaction at 198 MeV obtained by Yen *etal* [25] at average angles of 1.8° and 6.4°.

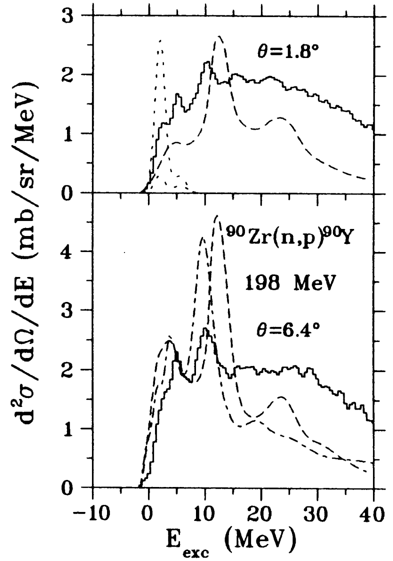

Fig. 7. Cross sections for the ^{90}Zr(n,p) reaction at 198 MeV. The theoretical curves correspond: to GT strength calculated by Bloom *etal* [26] (short-dashed lines in the upper panel); to the (1p1h) RPA of Klein *etal* [27] (long-dashed lines); to the RPA with (2p2h) correlations by Wambach *etal* [28] (dot-dashed lines in the lower panel).

The tall and short dotted lines in the upper spectrum represent GT strength calculated with different shell model assumptions by Bloom *etal* [26]. The dashed lines represent the 0° and 5° (1p1h) RPA calculation of Klein *etal* [27], whereas the dot-dashed curve from Wambach *etal* [28] includes the effects of (2p2h) correlations. There is little evidence for GT strength below 10 MeV. A safe upper limit of $S_+ \leq 3.6$ is obtained if the unrealistic assumption is made that all the cross section is L = 0; a more realistic upper limit, $S_+ \leq 1.6$, is obtained from the difference between the data and the calculation of Klein *etal* [27] which does not include GT stength. These upper limits are small when compared to the sum rule value of 30. Of special interest is the fact that the (2p2h) calculations produce too little damping of the spin–dipole resonance apparent in the 6.4° spectrum, and underestimate the data above $E_x \sim 18$ MeV. One may speculate that this could be remedied if correlations in the ^{90}Zr ground state (the RPA calculations assume a doubly closed shell) were included.

GAMOW–TELLER STRENGTH FUNCTIONS AND OTHER PHYSICS

GT strength functions are of special interest for other fields of physics. We mention briefly (i.e. without giving adequate references) three topics which are presently being addressed by nucleon scattering experiments at TRIUMF.

1. ASTROPHYSICS. In models of supernova explosions electron capture rates for nuclei in the iron region are important parameters. Electron capture which involves the S_+ strength function reduces the pressure of the relativistic electron gas and determines i) the rate at which gravitational collapse proceeds, ii) the mass M_i at the beginning of collapse, and iii) the mass M_h of the homologous core of maximum density. Difficulties in producing supernova explosions in the models which arise from energy absorption in remnant matter of the mantle of mass $(M_i - M_h)$ might be resolved if sufficient data on S_+ strength functions become available.

2. DOUBLE BETA DECAY. Double beta decay rates are dominated by the weak interaction process in which two neutrinos are emitted. The rates are governed by a coherent product of GT matrix elements involving 1^+ states in the intermediate odd–odd nucleus. These matrix elements can be studied independently by (p,n) and (n,p) experiments. Since S_+ strength is subject to severe Pauli blocking the (n,p) reaction may provide the key explanation why calculated lifetimes tend to be shorter than experiment, e.g. in ^{82}Se and ^{130}Te.

3. EXCHANGE CURRENTS. In $T_3 = 0$ nuclei such as ^{6}Li or ^{12}C GT matrix elements may be measured accurately by nucleon scattering if experiments to calibrate $\sigma/B(GT)$ are also carried out. Comparison of GT, and of M1 matrix elements from (e,e′) work, may help to identify meson exchange contributions which are expected to be small for an axial vector (GT) current, but large for a vector (M1) current (see the article by I.S. Towner in this volume).

CONCLUSIONS

We have shown that nucleon–nucleus scattering experiments between 200 and 400 MeV provide a quantitative, optimal tool to investigate the spin and isospin structure of the nuclear response. The GT component of the response at low energies is found to be reduced compared to most nuclear models, however the amount of quenching depends sensitively on the model assumptions made about the Fermi surface, especially for the S_+ strength. Although the question regarding the quenching mechanism is not yet completely resolved, it appears now likely that (2p2h) correlations are chiefly responsible for shifting GT strength to higher energies. Supporting evidence for this view comes from the large fraction of the sum rule observed in ^{54}Fe, from the small amount of GT strength found at low excitation in the $^{90}\mathrm{Zr}(n,p)$ reaction, and from the success of the slab model with (2p2h) corrections in reproducing large-angle spectra in $(\vec{p},\vec{p}')$ and (n,p) reactions on ^{54}Fe. A puzzling aspect of the data is the excess of (spin–transfer) strength in the high–energy region for both $^{54}\mathrm{Fe}(\vec{p},\vec{p}')$ and $^{90}\mathrm{Zr}(n,p)$ reactions over calculations which include (2p2h) components in the RPA. We speculate that this discrepancy might be remedied when correlations in the ^{54}Fe and ^{90}Zr ground states are considered.

REFERENCES

1. G.F. Bertsch and I. Hamamoto, Phys. Rev. C26, 1323 (1982).
2. G.E. Brown and M. Rho, Nucl. Phys. A372, 397 (1981).
3. C.D. Goodman *et al.*, Phys. Rev. Lett. 44, 1755 (1980).
4. T.N. Taddeucci *et al.*, Nucl. Phys. A469, 125 (1987).
5. O. Häusser *et al.*, Nucl. Instr. Meth. A254, 67 (1987).
6. R.L. Helmer, Can. J. Phys. 65 (1987), in press.
7. R.S. Henderson *et al.*, Nucl. Instr. Meth. A257, 97 (1987).
8. C. Gaarde *et al.*, Nucl. Phys. A334, 248 (1980).
9. K.P. Jackson *et al.*, submitted to Phys. Lett. *B*.
10. M.A. Franey and W.G. Love, Phys. Rev. C31, 488 (1985).
11. O. Häusser *et al.*, submitted to Phys. Rev. *C*.
12. B.H. Wildenthal, Progress in Particle and Nuclear Physics *Vol.*11, (Oxford: Pergamon 1984) p.5; and B.A. Brown, private communication.
13. W. Chung , PhD thesis, Michigan State University, 1976.
14. W.P. Alford *et al.*, to be published.
15. R.S. Sawafta *et al.*, submitted to Phys. Lett. *B*.
16. R.D. Madey *et al.*, Phys. Rev. C35, 2011 (1987).
17. M.C. Vetterli *et al.*, Phys. Rev. Lett. 59, 439 (1987); and to be published.
18. O. Häusser *et al.*, to be published.
19. J.R. Rapaport *et al.*, Nucl. Phys. A410, 371 (1983).
20. N. Auerbach *et al.*, Phys. Lett. B118, 256 (1982).
21. H. Esbensen and G. Bertsch, Ann. Phys. 157, 255 (1984).
22. R.D. Smith, private communication.
23. M. Moinester, Can. J. Phys. 65 (1987), in press.
24. R.D. Smith and J. Wambach, preprint.
25. S. Yen *et al.*, submitted to Phys. Lett. *B*.
26. S.D. Bloom, G.J. Mathews and J.A. Becker, Can. J. Phys. 65 (1987), in press.
27. A. Klein, W.G. Love and N. Auerbach, Phys. Rev. C31, 710 (1985).
28. J. Wambach, S. Drozdz, A. Schulte and J.A. Becker, preprint.